

Conformal Mapping on Rough Boundaries II: Applications to bi-harmonic problems

Damien Vandembroucq^(1,2) and Stéphane Roux^{(2)*}

(1) *Department of Applied Mathematics and Theoretical Physics
Cambridge CB3 9EW, UK*

(2) *Laboratoire de Physique et Mécanique des Milieux Hétérogènes,
Ecole Supérieure de Physique et de Chimie Industrielles,
10 rue Vauquelin, 75231 Paris Cedex 05, France*

We use a conformal mapping method introduced in a companion paper [1] to study the properties of bi-harmonic fields in the vicinity of rough boundaries. We focus our analysis on two different situations where such bi-harmonic problems are encountered: a Stokes flow near a rough wall and the stress distribution on the rough interface of a material in uni-axial tension. We perform a complete numerical solution of these two-dimensional problems for any univalued rough surfaces. We present results for sinusoidal and self-affine surface whose slope can locally reach 2.5. Beyond the numerical solution we present perturbative solutions of these problems. We show in particular that at first order in roughness amplitude, the surface stress of a material in uni-axial tension can be directly obtained from the Hilbert transform of the local slope. In case of self-affine surfaces, we show that the stress distribution presents, for large stresses, a power law tail whose exponent continuously depends on the roughness amplitude.

PACS numbers: 02.70.-c, 46.30.Cn, 47.15.Gf

I. INTRODUCTION

In a companion paper[1], we have presented a conformal mapping technique that allows us to map any 2D medium bounded by a rough boundary onto a half-plane. This method is based on the iterative use of FFT transforms and is extremely fast and efficient provided that the local slope of the interface remains lower than one. When the maximum slope exceeds one this algorithm, similar in spirit to a direct iteration technique well suited to circular geometries[2, 3], can no longer be used in its original form. Underrelaxation[4] suffices however to make it convergent for boundaries having large slopes. Beyond the determination of a conformal mapping for a given rough interface we have also shown in Ref.[1] how to generate directly mappings onto self-affine rough interfaces of chosen roughness exponent. Self-affine formalism is an anisotropic scaling invariance known to give a good description of real surfaces such as fracture surfaces[5, 6, 7]. This statistical property of fracture surfaces is of great interest in the study of friction or transport processes in geological faults[8, 9].

Building a conformal mapping is entirely equivalent to solving a harmonic problem with a uniform potential (or field) condition on the boundary. We used extensively this property in Ref.[1] to study stationary heat flows in the vicinity of a rough boundary and we focussed on the case of self-affine surfaces where we were able to com-

pute the exact correlation between local surface field and height profile. We gave also a special emphasis to the problem of the location of the plane interface equivalent to the rough one at infinity. It turned out that the conformal mapping technique provides a very direct means of computing the shift between the plane equivalent interface and the mean plane of the rough interface.

The range of applications of this first study naturally covers fields where Laplace equation appears: electrostatics, concentration diffusion, antiplane elasticity... In this second paper, we are specifically concerned with the case of bi-harmonic problems. The method we propose leads to the solution of the bi-harmonic field through the inversion of a linear system, as most other alternative numerical approaches (e.g. boundary elements method, spectral method...) but in contrast to the latters, the linear system to invert is naturally well conditioned and of rather modest size (N equations for N Fourier modes in the conformal mapping method) in contrast with direct spectral methods ($4N$ unknowns).

Moreover, following the first step of our algorithm analytically allows to obtain systematic perturbation expansion results.

After recalling our main results about conformal mapping in the first section, we deal successively with two important examples of bi-harmonic problems: Stokes flows and plane elasticity. The second section is thus devoted to the study of a stationary Stokes (*i.e.* low Reynolds number) flow close to a rough boundary. We shall also develop in this section the paradigm of the equivalent “no-slip” plane interface. In the third section we point out the problem of the stress distribution in a two-dimensional material bounded by a rough boundary and submitted

*present address Unité Mixte CNRS/Saint-Gobain, 39 Quai Lucien Lefranc 93303 Aubervilliers FRANCE; Electronic address: damien.vdb@saint-gobain.com, stephane.roux@saint-gobain.com

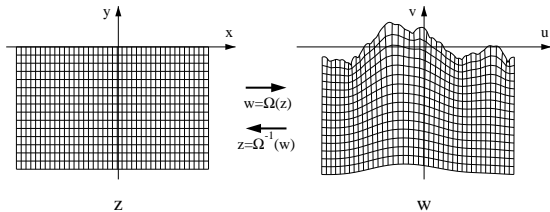


FIG. 1: A schematic illustration of the mapping Ω which maps the semi-infinite plane \mathcal{D} onto the domain limited by a rough interface \mathcal{E} .

to a uni-axial tension. The study of such situations is of particular interest for computing the influence of the roughness on the rupture probability law of brittle materials. We show that this problem is formally identical to that previously solved for the Stokes flow. We pay further a special attention to the case of self-affine surfaces and we present in this section numerical results that suggest that for large stresses, the surface stress statistical distribution law presents a power law behavior.

II. CONFORMAL MAPPING ON ROUGH BOUNDARIES

We recall here the essential results described in Ref. [1]. The aim of this section is to conformally map a half-plane onto a two-dimensional domain bounded by a rough interface. We first recall briefly how to build a conformal mapping well-suited to a given rough interface. This problem can be written under form similar as that of a “Theodorsen problem” [3]; in the semi-infinite geometry we deal with, it can be solved with an iterative algorithm using fast Fourier transforms [1]. The second part of this section is focussed on the specific case of self-affine interfaces. It turns out, indeed, that very simple constraints on a conformal mapping allow to generate directly a two-dimensional domain bounded by a self-affine interface of chosen roughness exponent. This property is of particular interest in statistical studies. We could thus establish in Ref.[1] the correlation between the norm of a harmonic field at a self-affine interface and the height of this latter.

A. Notations

As illustrated in Fig. 1, we are seeking for a mapping from a half-plane onto a two-dimensional domain bounded by a rough interface. In the following we place our study in the framework of the complex analysis. We consider then the lower half-plane \mathcal{D} whose complex coordinate $z = x + iy$ is such that $\Im m z \leq 0$ and the two-dimensional domain \mathcal{E} bounded by the rough interface $\partial\mathcal{E}$, we call $w = u + iv$ the complex coordinate in \mathcal{E} . We are seeking for a mapping Ω from \mathcal{D} onto \mathcal{E} . We restrict

our study to mappings Ω that are bijective holomorphic functions, *i.e.* Ω only depends on the variable z and not on its conjugate $\bar{z} = x - iy$. The transformations associated with such functions are said to be conformal in the sense that they preserve locally the angles. Let us now take advantage of the semi-infinite geometry we have to deal with. The two domains we consider are very similar apart from the region close to the boundary. Far from this one, Ω is essentially the Identity and we can write:

$$\Omega(z) = z + \omega(z), \quad (1)$$

where the perturbation ω decreases with depth and takes non negligible values only in the close vicinity of the interface. In the following, we consider periodic interfaces in order to minimize edge-effects. Without loss of generality, let us choose 2π to be the lateral period. A natural form of Ω is then:

$$\Omega(z) = z + \omega(z) = z + \sum_{k=0}^{\infty} \omega_k e^{-2ikz}. \quad (2)$$

where ω is expanded on a basis of evanescent modes.

B. Computing the mapping for an imposed interface

We consider a single valued interface $\partial\mathcal{E}$. Let h be the real function giving the interface geometry, for all point $w = u + iv$ of $\partial\mathcal{E}$,

$$v = h(u). \quad (3)$$

The mapping function Ω is such that $\Omega(\partial\mathcal{D}) = \partial\mathcal{E}$, *i.e.*

$$h(u) = \Im m \left(\sum_{k=0}^{\infty} \omega_k e^{-ikx} \right), \quad (4)$$

where $u = x + \Re e \left(\sum_{k=0}^{\infty} \omega_k e^{-ikx} \right).$

The first equation is here very close to a Fourier transform except that we have $h(u)$ instead of just $h(x)$ in the first term. This formal proximity can be used to build an iterative algorithm. For sufficiently small roughness, we can see from the second equation that x is an approximation of u at zeroth order. A direct Fourier transform of the profile $h(x)$ allows then a first approximation $\{\omega_k^{(0)}\}$ of the coefficients ω_k . The latter can be used to correct the previous approximation of $u(x)$, using (4b) gives then a following estimation of the non-uniform sampling $u(x)$ and of the coefficients ω_k via the Fourier transform of $h[u(x)]$. In appendix A, we give a more formal presentation of this algorithm. It turns out that this iterative technique converges provided that the maximum slope of the profile remains below unity. The technique can be used for any rough single-valued interface. For profiles whose maximum slope exceeds one, the algorithm can be

made convergent with slight modifications such that the use of under-relaxation techniques. We refer the reader to Ref. [1] for more details on the convergence and the stability analysis in this specific framework. Extensive studies of this technique in case of circular geometry are available in Ref. [2, 4].

C. Conformal mapping on self-affine interfaces

As pointed out above, the algorithm we have just described is suited to any rough interface. It is in particular possible to build conformal mappings associated with self-affine interfaces. The latter are defined by their scaling invariance properties: an interface described by the equation $y = h(x)$ is said to be self-affine if it remains (statistically) invariant under the transformations

$$\begin{cases} x \rightarrow \lambda x, \\ y \rightarrow \lambda^\zeta y, \end{cases} \quad (5)$$

for all values of the real parameter λ . The exponent ζ is called the ‘‘Hurst’’ or roughness exponent. It is characteristic of the scaling invariance. From this property, we derive easily that

$$\langle (h(x) - h(x + \delta))^2 \rangle = C^2 \delta^{2\zeta}, \quad (6)$$

where C is a prefactor. A simple Fourier transform gives then the power density spectrum of the rough self-affine profile.

$$P(k) \propto k^{-1-2\zeta}. \quad (7)$$

When using the algorithm previously described to map a self-affine interface, the first guess for the mapping function coefficients ω_k is thus such that:

$$\omega_k = 2ia_k \propto k^{-\frac{1}{2}-\zeta} x_k, \quad (8)$$

where the a_k are the coefficients of the Fourier transform of the profile and x_k are k independent random variables. It turns out that this power law behaviour is not altered by the following steps of the algorithm. In a symmetric way, we can impose, without any further restriction, the ω_k to follow a power law and have a look at the interface generated. We choose thus

$$\omega_k = A\epsilon_k k^{-1/2-\zeta}, \quad (9)$$

where ϵ_k are random Gaussian variable with 0 mean and unit variance for the real and imaginary part independently. We have however to note that nothing prescribes *a priori* that the function obtained is bijective. From the parametrical expression of the interface $\partial\mathcal{E}$, we can write

$$\Re \left[\frac{\partial \Omega}{\partial x}(x + i0) \right] = 1 + A \Im \left[\sum_k \epsilon_k k^{1/2-\zeta} e^{-ikx} \right], \quad (10)$$

and to guarantee that $\partial\mathcal{E}$ remains single-valued we have to choose amplitudes lower than the threshold value A_{max} where

$$A_{max} = \frac{-1}{\Im \left[\sum_k \epsilon_k k^{1/2-\zeta} e^{-ikx} \right]}. \quad (11)$$

We checked numerically (see Ref. [1]) that the power spectrum of such synthetic profiles was indeed a power law with the expected exponent.

III. STATIONARY STOKES FLOW IN THE VICINITY OF A ROUGH WALL

The Stokes equation describes fluid flows at low Reynolds numbers. We address in this section the problem of a stationary Stokes flow in the vicinity of a rough boundary. The study of such flows can be of great technological interest in the case of convective transport processes [12]: one can think of problems of surface deposition or erosion. In the same spirit, the occurrence of recirculating eddies can render very difficult the decontamination of a polluted surface; contaminants particles can be captured by diffusion in a cavity and remain trapped in it for an arbitrary long time. From a more fundamental point of view, in experiments consisting of tracing particles passively advected in a flow, the same process can lead to non gaussian statistics of the arrival time of tracer particles.

We consider a semi-infinite 2D geometry with periodic lateral boundary conditions and a unit shear rate at infinity. Far from being specific, the results obtained in this context can easily be extended for any case of stationary shear flow in the framework of a double scale analysis. Considering a shear flow of shear rate $\dot{\gamma}$ and an interface of typical boundary ε , where the velocity and pressure fields \mathbf{U} and p obey the usual Navier Stokes equation, we can, following Richardson [11], define an inner problem where the reduced non dimensional variables obey, at first order in ε , a simple Stokes equation in a semi-infinite geometry. In the following we present a solution of this Stokes equation that can be rewritten as a biharmonic equation for the stream function. This solution only requires the knowledge of a conformal mapping Ω from the lower half plane \mathcal{D} onto the actual space \mathcal{E} bounded by the rough interface $\partial\mathcal{E}$ and the inversion of a well conditioned linear system; it can thus be applied to any single-valued rough interface. We focus this brief study on the problem of the determination of the location of a plane boundary equivalent to the rough one at infinity. This problem is equivalent to the one of the replacement of the no-slip condition on a rough interface by a back flow condition (to be determined) on the mean plane. We compare our results with those of Tuck and Kouzoubov [10] who developed in the *actual space* a method similar to ours in spirit. Recent results about Stokes flows near rough boundaries can also be found in

references [12, 13, 14]; in most of them the Stokes equation is solved using boundary elements methods (see for instance the review of Pozrikidis [15]).

A. General solution

We address here the problem of a unit shear Stokes flow in the vicinity of a rough boundary. Let us call $\Psi(w)$ the stream-function associated to the velocity field \mathbf{b} in the actual space \mathcal{E} . We have by definition

$$b_u = \frac{\partial \Psi}{\partial v}, \quad b_v = -\frac{\partial \Psi}{\partial u}. \quad (12)$$

In a stream function formalism, the Stokes equation is reduced to a simple bi-harmonic equation. Taking into account the boundary conditions *i.e.* no slip on the interface and unit shear rate at infinity, $\Psi(w)$ has to be solution of the following problem:

$$\begin{cases} \nabla_w^4 \Psi(w) = 0 & \text{in } \mathcal{E} \\ \nabla_w \Psi(w) = \mathbf{0} & \text{on } \partial \mathcal{E} \\ \Psi(w) \sim \frac{1}{2}v^2 & \text{as } v \rightarrow -\infty \end{cases} \quad (13)$$

The essential difficulty obviously lies in the no slip condition on the interface ; the use of a conformal mapping allows us to build an equivalent problem with a much easier boundary condition, the new interface being plane instead of rough. Let us associate to the stream-function Ψ in the actual space \mathcal{E} the real potential Φ in the half-plane \mathcal{D} :

$$\Phi(z) = \Psi \circ \Omega^{-1}(w), \quad (14)$$

where Ω maps \mathcal{D} onto \mathcal{E} . We can thus define the following equivalent problem in the new geometry:

$$\begin{cases} \nabla_w^4 \Psi(w) = 0 \\ \nabla_w \Psi(w) = 0 & \text{on } \partial \mathcal{E} \\ \Psi(w) \sim \frac{1}{2}v^2 & \text{as } v \rightarrow -\infty \end{cases} \quad (15)$$

$$\Leftrightarrow \begin{cases} \nabla_z^2 \left[\frac{\nabla_z^2 \Psi(z)}{|\Omega'(z)|^2} \right] = 0 \\ \nabla_z \Phi(z) = 0 & \text{on } \partial \mathcal{D} \\ \Phi(z) \sim \frac{1}{2}y^2 & \text{as } y \rightarrow -\infty \end{cases}$$

In the case of a simple harmonic equation, building the conformal mapping gives immediately the complete solution; this is unfortunately no longer true in the case of a bi-harmonic equation. One can see that the original equation is changed into a linear equation with non-constant coefficients. The latter equation is directly related to the mapping function Ω . We show in the following that this difficulty can be circumvented. Let us recall that in addition to the above described conditions, the new potential Φ has to be real and 2π -periodic in x . Besides, the boundary condition can be made simpler taking into account that the interface is now plane. Φ

being defined apart from an additive constant, we can write that it obeys:

$$\nabla_z \Phi = \mathbf{0} \quad \text{on } \partial \mathcal{D} \Leftrightarrow \begin{cases} \Phi = 0 & \text{on } \partial \mathcal{D} \\ \frac{\partial \Phi}{\partial y} = 0 & \text{on } \partial \mathcal{D} \end{cases}. \quad (16)$$

The bi-harmonic potential Φ can always be written in terms of two holomorphic functions F and H such that:

$$\Phi(z) = \Omega(z)\bar{F}(z) + F(z)\bar{\Omega}(z) + H(z) + \bar{H}(z). \quad (17)$$

In the following we split both functions into a purely periodic part (denoted by the index p) and a non-periodic part. Taking into account the desired behaviors at infinity provides:

$$\begin{aligned} F(z) &= \frac{1}{8}z + F_p(z), \\ H(z) &= -\frac{1}{8}z^2 + H_1(z) + H_p(z), \end{aligned} \quad (18)$$

with

$$F_p(z) = \sum_{n \geq 0} f_n e^{-inz}, \quad H_p(z) = \sum_{n \geq 0} h_n e^{-inz}, \quad (19)$$

and H_1 is z times a x -periodic function. The lateral periodicity of Φ forbids the occurrence of terms proportional to polynoms of the real variable x , hence:

$$H_1(z) = -z \left(F_p(z) + \frac{1}{8}\omega(z) \right), \quad (20)$$

and Φ becomes then:

$$\begin{aligned} \Phi(z) &= \frac{1}{2}y^2 + \sum_n h_n e^{-inz} + \sum_n \bar{h}_n e^{in\bar{z}} \\ &+ 2iy \sum_n \left(\bar{f}_n + \frac{1}{8}\bar{\omega}_n \right) e^{in\bar{z}} \\ &- 2iy \sum_n \left(f_n + \frac{1}{8}\omega_n \right) e^{-inz} \\ &+ \sum_{n \geq 1} \sum_p (f_p \bar{\omega}_{n+p} + \omega_p \bar{f}_{n+p}) e^{inx} e^{(n+2p)y} \\ &+ \sum_{n \geq 1} \sum_p (\bar{\omega}_p f_{n+p} + \bar{f}_p \omega_{n+p}) e^{-inx} e^{(n+2p)y} \\ &+ \sum_n (\omega_n \bar{f}_n + \bar{\omega}_n f_n) e^{2ny}. \end{aligned} \quad (21)$$

We can deduce from the latter expression the partial derivative of Φ with y :

$$\begin{aligned} \frac{\partial \Phi}{\partial y}(z) &= y + \sum_n n h_n e^{-inz} + \sum_n n \bar{h}_n e^{in\bar{z}} \\ &+ 2iy \sum_n n \left(\bar{f}_n + \frac{1}{8}\bar{\omega}_n \right) e^{in\bar{z}} - 2iy \sum_n n \left(f_n + \frac{1}{8}\omega_n \right) e^{-inz} \\ &+ 2i \sum_n \left(\bar{f}_n + \frac{1}{8}\bar{\omega}_n \right) e^{in\bar{z}} - 2i \sum_n \left(f_n + \frac{1}{8}\omega_n \right) e^{-inz} \\ &+ \sum_{n \geq 1} \sum_p (n+2p) (f_p \bar{\omega}_{n+p} + \omega_p \bar{f}_{n+p}) e^{inx} e^{(n+2p)y} \\ &+ \sum_{n \geq 1} \sum_p (n+2p) (\bar{\omega}_p f_{n+p} + \bar{f}_p \omega_{n+p}) e^{-inx} e^{(n+2p)y} \\ &+ \sum_n 2n (\omega_n \bar{f}_n + \bar{\omega}_n f_n) e^{2ny}. \end{aligned} \quad (22)$$

The holomorphic functions Ω_p , F_p and H_p being 2π -periodical, they can be developed using the basis of the functions $\{e^{-ikz}\}$. Besides, the interface $\partial\mathcal{D}$ being simply the x -axis, the restriction of these holomorphic functions to the boundary can be written in $\{e^{-ikx}\}$. The boundary condition problem can then be written by cancelling out the projections of Φ and $\partial_y\Phi$ on the functions-vectors $\{e^{-ikx}\}$. Keeping only the first N modes, we obtain $2N$ equations which allow to obtain the $2N$ components f_n and h_n . The projection of the boundary condition on the function-vector 1 ($k = 0$) gives first:

$$\begin{cases} \Phi : & \sum_n (\omega_n \bar{f}_n + \bar{\omega}_n f_n) + h_0 + \bar{h}_0 = 0, \\ \partial_y \Phi : & \sum_n 2n (\omega_n \bar{f}_n + \bar{\omega}_n f_n) + 2i \left(\bar{f}_0 + \frac{1}{8} \bar{\omega}_0 \right) \\ & - 2i \left(f_0 + \frac{1}{8} \omega_0 \right) = 0. \end{cases} \quad (23)$$

We have then for the function-vectors $\{e^{-ikx}\}$ with $k \neq 0$:

$$\begin{cases} \Phi : & \sum_p (\bar{\omega}_p f_{k+p} + \bar{f}_p \omega_{k+p}) + h_k = 0, \\ \partial_y \Phi : & \sum_p (k+2p) (\bar{\omega}_p f_{k+p} + \bar{f}_p \omega_{k+p}) + k h_k \\ & - 2i \left(f_k + \frac{1}{8} \omega_k \right) = 0. \end{cases} \quad (24)$$

We can thus write the following linear system:

$$\begin{cases} f_k + \frac{1}{8} \omega_k + i \sum_p p (\bar{\omega}_p f_{k+p} + \bar{f}_p \omega_{k+p}) = 0, \\ h_k = - \sum_p (\bar{\omega}_p f_{k+p} - \bar{f}_p \omega_{k+p}). \end{cases} \quad (25)$$

The coefficients $\{f_k\}$ are solutions of the first equation, a $N \times N$ linear system. The coefficients $\{h_k\}$ are easily deduced from the $\{f_k\}$. Once the conformal mapping is known, the numerical resolution of the Stokes equation just requires the inversion of the linear system. Let us note that the latter system is easy to invert, which would not have been the case if we have written the boundary condition in the w -space. The latter method was recently used by Tuck et Kouzoubov [10]. In the cited reference, they use expansions in a basis of $\{e^{-ky} \cos(kx)\}$ and write a linear system discretizing the rough interface in N points. If this method is efficient in the small slope limit, it becomes however unpracticable for large slopes. The procedure requires thus the numerical inversion of a matrix consisting of terms of order $e^{\pm NA}$ where A is the roughness amplitude and this becomes practically difficult or unprecise as soon as the product NA increases. The conformal mapping avoids such numerical difficulties since the boundary is plane in the equivalent domain. One can see on figures 2 and 3 maps of the stream function for a stationary Stokes flow for two rough surfaces identical up to a dilation of factor 4 in the vertical direction. The stream lines closely follow the smooth interface

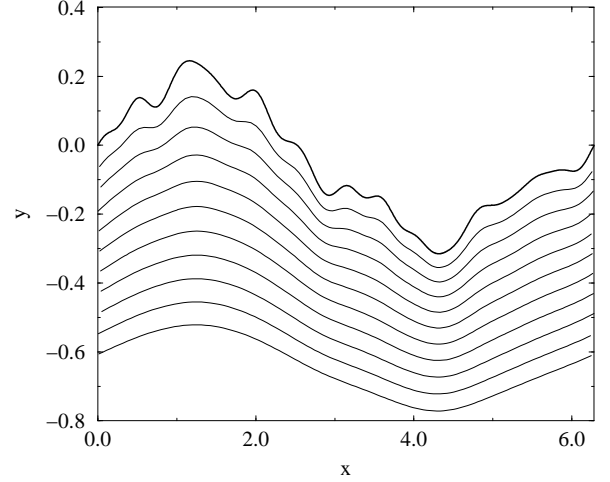


FIG. 2: Stream lines of a Stokes flow along a rough surface.

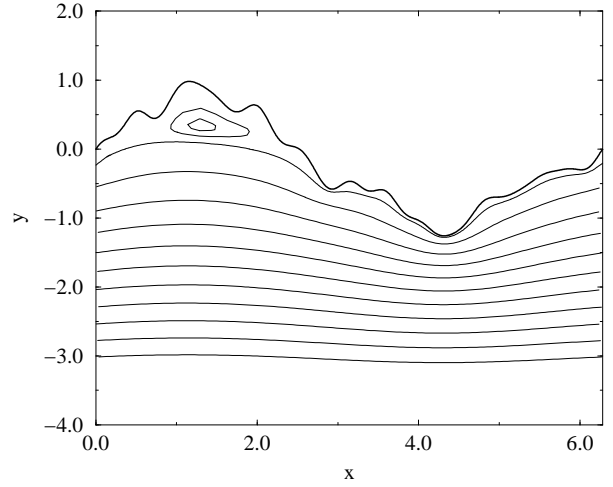


FIG. 3: Stream lines of a Stokes flow along the same rough surface as above but four times rougher. We observe that a recirculation flow appears in the deepest cavity.

(Fig. 2) while an eddy appears in the largest depression of the roughest interface (Fig. 3).

B. Equivalent plane boundary

We now introduce the notion of an equivalent plane no-slip boundary in the framework of a stationary Stokes flow. Our aim is here to replace the no-slip condition on the rough boundary by a no slip condition on an equivalent plane boundary, the stream function remaining unchanged at infinity. Let us recall that like in the case of a rough electrode which was studied in Ref. [1], noth-

ing prescribes the plane equivalent boundary to lie at the average height of the rough one. In harmonic problems, the dissymmetry between peaks and cavities due to point effects leads the equivalent plane boundary to be shifted towards the peaks. We shall see in the following that the same conclusion holds in the case of the stationary Stokes flow. An illustration of this dissymmetry naturally emerges with the occurrence of little eddies in pronounced depressions of the rough boundary. We have chosen in this text to develop the paradigm of no-slip plane equivalent boundary but it is naturally also possible to consider a plane boundary fixed at the average plane with a roughness dependent slip boundary. The conclusion previously mentioned about the place of the equivalent boundary (nearer from the peaks than from the cavities) is then expressed by a reversal flow condition. We show in the following that the conformal mapping method gives a natural way to compute the vertical shift of the plane equivalent boundary. We compare these results with a perturbative solution that can be directly computed from the Fourier coefficients of the interface.

1. Conformal mapping approach

As already mentioned, the stream function $\Psi(u, v)$ of the Stokes flow is entirely determined by the following conditions:

$$\begin{cases} \nabla_w^4 \Psi(w) = 0 & \text{in } \mathcal{E} \\ \nabla_w \Psi(w) = \mathbf{0} & \text{on } \partial\mathcal{E} \\ \Psi(w) \sim \frac{1}{2}v^2 & \text{as } v \rightarrow -\infty \end{cases} \quad (26)$$

If we now return to the solution obtained via conformal mapping, we have:

$$\begin{aligned} \Phi(z) = & \frac{1}{2}y^2 + \sum_n h_n e^{-inz} + \sum_n \bar{h}_n e^{in\bar{z}} \\ & + 2iy \sum_n \left(\bar{f}_n + \frac{1}{8}\bar{\omega}_n \right) e^{in\bar{z}} \\ & - 2iy \sum_n \left(f_n + \frac{1}{8}\omega_n \right) e^{-inz} \\ & + \sum_{n \geq 1} \sum_p (f_p \bar{\omega}_{n+p} + \omega_p \bar{f}_{n+p}) e^{inx} e^{(n+2p)y} \\ & + \sum_{n \geq 1} \sum_p (\bar{\omega}_p f_{n+p} + \bar{f}_p \omega_{n+p}) e^{-inx} e^{(n+2p)y} \\ & + \sum_n (\omega_n \bar{f}_n + \bar{\omega}_n f_n) e^{2ny} . \end{aligned} \quad (27)$$

By construction, $\Phi(z)$ is such that $\Psi(w)$ is bi-harmonic in \mathcal{E} and fulfills the no-slip boundary condition at the rough interface. Let us now build the stream function Ψ_{eq} associated with a plane interface located at $v = H$; we have immediatly:

$$\Psi_{eq}(w) = \frac{1}{2}(v - H)^2, \quad (28)$$

and its associated function in the half-plane \mathcal{D} is

$$\Phi_{eq}(z) = \frac{1}{2}[\Im m \Omega(z) - H]^2, \quad (29)$$

that becomes at infinity:

$$\begin{aligned} \Phi(z) &= \frac{1}{2}y^2 + \frac{1}{2}y \Im m(\omega_0 + 8f_0) + \mathcal{O}(1) \quad \text{as } y \rightarrow -\infty, \\ \Phi_{eq}(z) &= \frac{1}{2}y^2 + y[\Im m(\omega_0) - H] + \mathcal{O}(1) \quad \text{as } y \rightarrow -\infty. \end{aligned} \quad (30)$$

Taking into account Eq.(23) which specifies the expression of f_0 , the identity between Φ and Φ_{eq} defines the value of H

$$H = \Im m(\omega_0) + 2 \sum_n n (\omega_n \bar{f}_n + \bar{\omega}_n f_n). \quad (31)$$

2. Perturbative approach

Let us consider an interface of amplitude, say A , with characteristic length λ such that the profile is statistically symmetrical. When we seek for the location of the plane equivalent electrode, we expect two different behaviors i) a dependence on A^2/λ in case of small amplitude or low spatial frequency ii) a linear dependence on A in case of large amplitude or high spatial frequency. The latter behavior comes directly from the fact that the equivalent plane reaches at maximum the level of the highest peaks. In case of small slopes, it is easy to show that the correction from the average plane is of order A^2/λ . The deviation H is naturally normalized by the amplitude of roughness A . The ratio H/A has then to be a function of the two only characteristic lengths of the system, A and λ and can be expanded in the limit of small slopes:

$$\frac{H}{A} = \phi\left(\frac{A}{\lambda}\right) = a_0 + a_1 \frac{A}{\lambda} + a_2 \left(\frac{A}{\lambda}\right)^2 + \mathcal{O}\left(\frac{A}{\lambda}\right)^3. \quad (32)$$

A simple symmetry about the mean plane has to leave H unchanged, since this symmetry is equivalent to a transformation of A into $-A$, a_0 and a_2 have to be zero and:

$$H = a_1 \frac{A^2}{\lambda} + \mathcal{O}\left(\frac{A^4}{\lambda^3}\right) \quad (33)$$

A detailed perturbative analysis can be built in the case of a simple sine interface [10]. Writing a perturbative solution in the conformal mapping formalism allows us to deal with any rough interface. Following (21) we have:

$$\begin{aligned} \Phi(z) = & \frac{1}{2}y^2 + 4y \Im m \left(F_p(z) + \frac{1}{8}\omega(z) \right) \\ & + 2\Re e \left(\omega(z) \overline{F_p(z)} + H_p(z) \right). \end{aligned} \quad (34)$$

By construction, ω , F_p and H_p are of order A , A being the roughness amplitude. At first order the no-slip boundary condition becomes:

$$\begin{aligned} \Phi(x) = 0 & \iff \Re e \left(H_p^{(1)}(x) \right) = 0, \\ \frac{\partial \Phi}{\partial y}(x) = 0 & \iff 4\Im m \left(F_p^{(1)}(x) + \frac{1}{8}\omega^{(1)}(x) \right) \\ & + 2\Re e \left(\frac{\partial H_p^{(1)}}{\partial y}(x) \right) = 0. \end{aligned} \quad (35)$$

The holomorphic functions being bounded, the resolution of these Hilbert problems gives immediatly:

$$H_p^{(1)}(z) = 0, \quad F_p^{(1)}(z) = -\frac{1}{8}\omega^{(1)}(z). \quad (36)$$

Using the iterative algorithm briefly presented in section II (see Appendix for details), a first order approximation of the coefficients ω_k is

$$\omega_k = i\frac{\tilde{h}_k}{N} + \mathcal{O}(A^2), \quad (37)$$

where $\{\tilde{h}\}$ is the $2N$ discrete Fourier transform of the real function h associated with the rough interface. Using the expression of $\Im m(\omega_0)$ derived in section V-B of Ref. [1], we can write:

$$H = -\frac{1}{N^2} \sum_{k>0} k |\tilde{h}_k|^2. \quad (38)$$

This result is consistent with the one proposed in Ref. [10] for a backflow slip condition on the mean plane of the interface. In the particular case of a pure sine profile of amplitude A and wavelength λ , we recover:

$$H = -2\pi \frac{A^2}{\lambda}. \quad (39)$$

It has to be noted these first order results are exactly identical to those obtained in the case of a rough electrode (up to a factor 2) despite the fact we had here to solve a biharmonic equation instead of a simple harmonic one. On figures 4 and 5 we have plotted both results of the perturbative solution and of the conformal mapping calculation in case of a sine interface and of a self affine interface of roughness exponent 0.8 built with 64 Fourier modes. We check that the perturbative calculations correctly fit the results for small slopes (up to 0.5). For larger slopes, the perturbative expression overestimates the deviation whose behavior becomes progressively linear. Note that our numerical method allowed us to reach local slope values up to 2.5. This maximum slope can be increased by using more Fourier modes in the mapping function (we used 256 modes in the present calculation).

IV. ELASTICITY

In this section, we analyse the effect of a slight surface roughness on the stress distribution in an elastic medium. We emphasize here the case of a semi-infinite material submitted to a uni-axial tension. Although very elementary, this simple model illustrates an effect which has been suggested to be responsible for the mechanical strength of glass fibers. Recent experimental results [16] suggest that the nanometric roughness at the surface of glass fibers of diameter a few micrometers could be responsible for the decrease of the tensile resistance by a

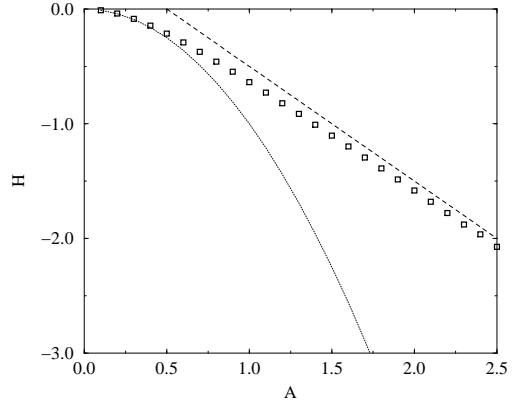


FIG. 4: Shift from the mean plane of the plane equivalent boundary for a Stokes flow in case of sine interface of varying amplitude A . The dotted line corresponds to the second order perturbative expansion and the symbols to computations using conformal mapping. The dashed line has a slope -1.

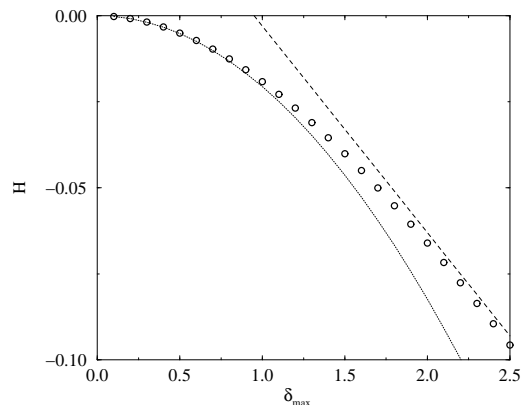


FIG. 5: Shift from the mean plane of the plane equivalent boundary for a Stokes flow in case of self-affine interface of varying amplitude. We use in abscissa the maximum local slope δ_{max} . The dotted line correspond to the second order perturbative expansion and the symbols to computations using conformal mapping. The dashed line has a slope -0.06. The surface has been built with 64 Fourier modes and we used 256 modes in the solution based on conformal mapping.

factor of about 5. In uniaxial tension, the resistance of a fiber is directly related to the distribution of maximum positive principal stresses. Using a simple perturbative expansion, we show that in the limit of small slopes, the surface stress can be directly computed from the Hilbert transform of the local slope.

The Weibull law [17] usually gives a correct description of failure statistics in a wide range of brittle materials. This phenomenological law is partly based on the identification of the weakest link in the material (whose size is supposed to be that of the smallest defects). We will

see in the following that for a self-affine surface (such as measured for glass fibers by AFM techniques [16]) the statistical distribution of tensile stresses at the boundary displays a power law behavior, which naturally implies the validity of Weibull statistical failure distribution. Moreover the exponent of this power law, *i.e.* the Weibull modulus, continuously depends on the roughness amplitude.

A. General solution

In plane stress or plane strain conditions, the stress tensor $[\sigma]$ can be completely represented by a unique real function, named the Airy function:

$$[\sigma] = \begin{bmatrix} \sigma_{uu} & \sigma_{uv} \\ \sigma_{uv} & \sigma_{vv} \end{bmatrix} \quad \text{where} \quad \begin{cases} \sigma_{uu} = \frac{\partial^2 \Psi}{\partial v^2} \\ \sigma_{uv} = -\frac{\partial^2 \Psi}{\partial u \partial v} \\ \sigma_{vv} = \frac{\partial^2 \Psi}{\partial u^2} \end{cases} \quad (40)$$

This form directly comes from the stress balance in absence of external forces *i.e.* $\text{div}[\sigma] = 0$. In the framework of 2D elasticity in an isotropic medium, the Airy function obeys:

$$\Delta \Delta \Psi = 0 \quad \text{in } \mathcal{E}. \quad (41)$$

The stress tensor being computed from two successive derivations of the bi-harmonic function Ψ , the latter is only defined apart from a linear function in u and v . In the following, we consider free boundary conditions $[\sigma]\mathbf{n} = \mathbf{0}$ and we impose a uni-axial tension at infinity. Let \mathbf{n} denote a unit vector normal to the interface, we have:

$$\begin{cases} [\sigma]\mathbf{n} = \mathbf{0} & \text{on } \partial\mathcal{E}, \\ [\sigma] \rightarrow \begin{bmatrix} 1 & 0 \\ 0 & 0 \end{bmatrix} & \text{as } y \rightarrow -\infty. \end{cases} \quad (42)$$

The Airy function Ψ is thus such that:

$$\begin{cases} n_u \frac{\partial^2 \Psi}{\partial v^2} - n_v \frac{\partial^2 \Psi}{\partial u \partial v} = 0 & \text{on } \partial\mathcal{E}, \\ n_u \frac{\partial^2 \Psi}{\partial u \partial v} - n_v \frac{\partial^2 \Psi}{\partial u^2} = 0 & \text{on } \partial\mathcal{E}, \\ \Psi \sim \frac{1}{2}v^2 & \text{as } v \rightarrow -\infty. \end{cases} \quad (43)$$

At any point of the interface $\partial\mathcal{E}$, it is possible to give a parametric representation of the tangential and normal vectors \mathbf{t} and \mathbf{n} :

$$\mathbf{t}(w) = \frac{\Omega'(x)}{|\Omega'(x)|}, \quad \mathbf{n}(w) = \frac{i\Omega'(x)}{|\Omega'(x)|}. \quad (44)$$

The boundary conditions at the interface can be rewritten:

$$\begin{aligned} [\sigma]\mathbf{n} &= 0 & \text{on } \partial\mathcal{E} \\ \Leftrightarrow (\mathbf{t} \cdot \nabla_w) \nabla_w \Psi &= 0 & \text{on } \partial\mathcal{E} \\ \Leftrightarrow \nabla_w \Psi = Cst. &= 0 & \text{on } \partial\mathcal{E}. \end{aligned} \quad (45)$$

We can choose the constant to be zero since the Airy function is only defined apart from an affine function. This leads to:

$$\begin{aligned} \frac{\nabla_z \Phi}{\Omega'(z)} &= 0 & \text{on } \partial D \\ \Leftrightarrow \nabla_z \Phi &= 0 & \text{on } \partial D. \end{aligned} \quad (46)$$

It turns out that the boundary condition at the interface is exactly the same as the one we have encountered for the no-slip condition in a Stokes flow. The Airy function is thus identical to the above derived stream function for Stokes flow.

B. Surface stress distribution

1. Perturbative approach

The normal stress being zero at the interface, the first order expression derived in the previous section gives us the following result for the principal (tangential) stress at the interface:

$$\begin{aligned} \sigma_{tt} &= \Delta \Psi(w) = \frac{\Delta \Phi(x)}{|\Omega'(x)|^2} \\ &= 1 - 2\Re \left[\omega^{(1)'}(x) \right] \\ &= 1 - 2 \sum_{k=-n+1}^{k=n} i \frac{k}{|k|} (-ik) \frac{\widetilde{h}_k}{2n} e^{-ikx} \\ &= 1 - 2\mathcal{H}[\varphi'](x), \end{aligned} \quad (47)$$

where $\mathcal{H}[\dots]$ stands for the Hilbert transform operator on the real axis. At first order, we find that the tangential surface stress deviation from its mean value is proportional to the *Hilbert transform of the local slope*. Fig. 6 and 7 give two examples of stress distribution on surfaces of respectively maximum slope 0.1 and 0.4. In both cases, we can see that the stress fluctuations are much greater than the height fluctuations (which have been dilated by a factor 5 in the figures). Note that (taking into account the dilation of the height profile) the stress fluctuations are very large compared with those of the height. In the context of rupture, the relevant parameter being the maximum stress, one can understand that a very modest roughness can be responsible for a dramatic decrease of the material resistance.

We observe a good agreement between the stress profile computed by conformal mapping and the perturbative result (related to the Hilbert transform of the slope) for the smoothest interface but this is no longer the case for the roughest one especially in the area where the curvature is large. Higher order perturbative terms are thus necessary to recover the actual stress.

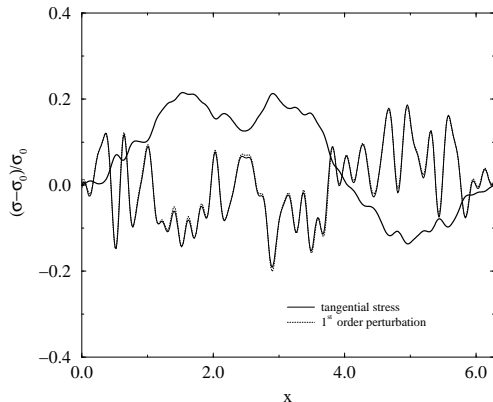


FIG. 6: Stress and height profiles on the rough interface of a 2D medium submitted to uni-axial tension. The bold line represents the height profile (of maximum slope 0.1) dilated by a factor 5. The solid line gives the stress distribution obtained by the complete conformal mapping computation, the dotted line is a first order expression of the stress which is directly obtained from the Hilbert transform of the local slope of the interface.

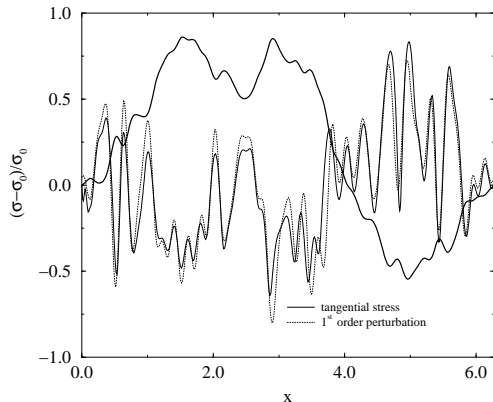


FIG. 7: Same figure as above with an interface four times rougher. One observes that in large curvature areas, the first order approximation does no longer suffice to represent precisely the local stress. The height profile (of maximum slope 0.4) dilated by a factor 5.

2. Statistical results

Let us now turn to the study of stress distributions on self-affine surfaces. The latter are designed to present a Gaussian height distribution *i.e.* their Fourier coefficients are $\widehat{h}_k = A\epsilon_k k^{-\frac{1}{2}-\zeta}$ where ϵ_k is a Gaussian random variable of zero mean and unit standard deviation. In case of small slopes, the validity of the first order perturbative result suggests thus that the stress distribution is Gaussian. On Fig. 8 we have plotted in log-log scale the surface stress distribution obtained for 1500 self-affine

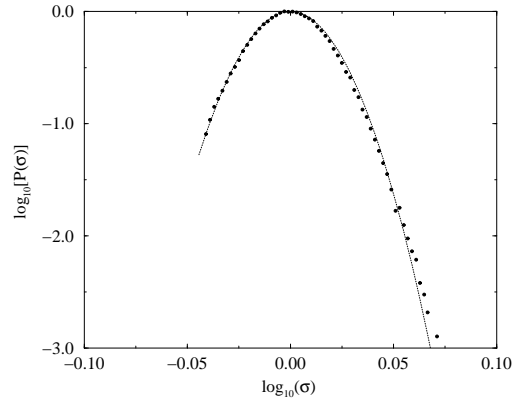


FIG. 8: Surface stress distribution for self-affine surfaces of roughness exponent $\zeta = 0.8$ and of roughness amplitudes $A = 0.05\epsilon_{max}$, ϵ_{max} is the amplitude such that the maximum local slope is equal to 1. The self-affine interfaces have been built with 32 Fourier modes and the results averaged on 1500 surfaces. We can check that the distribution (symbols) is well fitted by a parabola, which shows that the stress is log-normally distributed.

surfaces of roughness exponent $\zeta = 0.8$ and of maximum slope 0.05, one can check that, as expected, the distribution is well fitted by a parabola.

In case of larger slopes we have seen that the agreement between the first order perturbative results and the complete computation becomes poorer. We can then wonder if the log-normal behavior of the distribution is preserved. On Fig. 9, we have plotted the surface stress distribution for four self-affine surfaces of roughness exponent $\zeta = 0.8$ and of respective maximum slopes 0.2, 0.4, 0.6 and 0.8. These results were obtained by averaging the data obtained from 1000 different surfaces each defined with 64 Fourier modes. We can see a clear power law like behaviour for large stress amplitudes. The slopes we can measure are very dependent on the roughness amplitude. The interpretation of these new numerical results requires a perturbative analysis that we have not developed yet for this bi-harmonic problem. We have however performed a similar analysis in the case of a harmonic field on self-affine interfaces [18]. It turned out that in a similar fashion as the one presented above, the field distribution law present a power law tail with an exponent $\tau \propto A^{-2}\ell^{1-\zeta}$ where A is the roughness amplitude, ℓ the spatial lower cut-off of the self-affine domain and ζ the roughness exponent. Calling g the logarithm of the field, the latter result was derived showing that the reduced variable

$$f_A(g) = \left(\sqrt{1 + 2Kg} - 1 \right) / KA \quad (48)$$

follows a Gaussian distribution ($K \simeq 2$ for harmonic problems). Using $K = 0.25$, we can check indeed (see Fig. 10) that all data obtained from our calculations collapse on a same parabola in log-log scale. These nu-

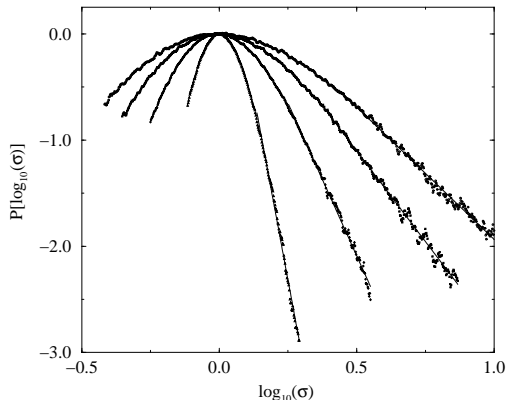


FIG. 9: Surface stress distribution for self-affine surfaces of roughness exponent $\zeta = 0.8$ and of roughness amplitudes $A = 0.2\epsilon_{max}$ (\triangle), $0.4\epsilon_{max}$ (\diamond), $0.6\epsilon_{max}$ (\square) and $0.8\epsilon_{max}$ (\circ), ϵ_{max} is the amplitude such that the maximum local slope is equal to 1. The self-affine interfaces have been built with 64 Fourier modes and the results averaged on 1000 surfaces. For each distribution, a bold line shows the power law behavior obtained for large stresses.

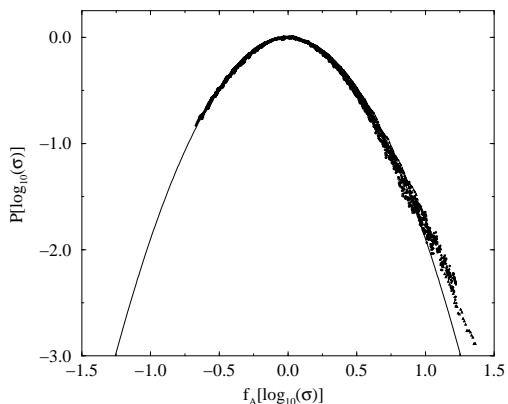


FIG. 10: Same distributions as in the previous figure in the reduced variable $f_A(g) = (\sqrt{1 + 2Kg} - 1) / KA$ where $g = \log_{10}(\sigma)$ and $K = 0.25$. The data collapse onto a simple parabola, which shows the Gaussian character of the distribution of $f_A(g)$

merical results indicate that a same scaling applies for both harmonic and bi-harmonic fields on self-affine surfaces. A detailed analysis of these statistical properties will be addressed elsewhere.

V. CONCLUSION

After introducing a conformal mapping technique that allowed for a detailed study of harmonic field in the vicinity of rough boundaries [1], we have extended in this pa-

per the use of this method to the study of bi-harmonic fields. We have given a general solution to problems such that the Stokes flow over a rough surface and the stress distribution in a medium (bounded by a rough interface) in uni-axial tension. Besides the knowledge of the mapping function (obtained using a simple iterative algorithm), this solution only requires the linear inversion of a well conditioned matrix. The determination of the mapping function being only limited by the maximum value of the local slope at the interface, the method is well suited to any kind of single-valued interface. As an illustration, we have thus presented results of Stokes flow over self-affine boundaries whose maximum slope reach 2.5. In the same context of a Stokes flow over a rough boundary, we pay a special attention to the determination of the location of an equivalent no-slip plane interface. The conformal mapping method gives way to a very natural determination of this quantity. A simple perturbative solution allowed us to retrieve for it a result proposed by Tuck and Kouzoubov [10]. In the context of the plane elasticity, the same perturbative result has allowed us to show that, in the limit of small slopes, the surface stress distribution was directly related to the Hilbert transform of the slope of the interface. This very simple result could be used e.g. for the evolution of a stress-corrosion front. The analysis of statistical results for the principal stress on self-affine surfaces has shown moreover that the large stress distribution presents a power law tail whose exponent continuously depends on the roughness amplitude. Such results could be applied in the context of glass fiber rupture statistics to provide a fundamental basis for the Weibull law that is known to describe accurately the rupture statistics. A realistic description of these stress distributions require a second order perturbative analysis which will be presented in a further study. We have, however, recently proposed such an approach in case of harmonic fields [18] where distributions of the same kind have also been found and justified in two and three dimensions.

Acknowledgements

It is a pleasure to acknowledge enlightning discussions with F. Creuzet, E.J. Hinch and J.R. Willis. We are also grateful to B. Forget and A. Tanguy for useful help and comments.

Appendix: Iterative algorithm

In this appendix we present the iterative scheme allowing us to build the conformal mapping $\Omega(z) = z + \sum_k \omega_k e^{-ikz}$ for any given single valued rough interface. As exposed in II.B, we are seeking for a mapping function Ω such that $\Omega(\partial\mathcal{D}) = \partial\mathcal{E}$, where $\partial\mathcal{E}$ is the rough interface and $\partial\mathcal{D}$ is the x-axis. The single valued interface $\partial\mathcal{E}$ being associated to the real function h , this

condition is rewritten:

$$h(u) = \text{Im} \left(\sum_{k=0}^{\infty} \omega_k e^{-2i\pi k z} \right), \quad (49)$$

where $u = x + \text{Re} \left(\sum_{k=0}^{\infty} \omega_k e^{-2i\pi k z} \right)$.

We build the algorithm in the following way: the intermediate quantities appearing at the k th iteration are labelled with a superscript (k) , all functions are decomposed over a set of $2n$ discrete values, the number of Fourier modes is thus limited to $2n$. We first introduce a series of sampling points $u_j^{(k)}$ with $j = 0, \dots, n-1$ which is initially set to an arithmetic series $u_j^{(0)} = j\pi/n$. The sampling of $h(u)$ by the $u_j^{(k)}$ gives the array:

$$h_j^{(k)} = h(u_j^{(k)}) \quad (50)$$

The discrete Fourier transform of this array is the complex valued array

$$a_j^{(k)} = \sum_{m=-n+1}^n h_m^{(k)} e^{imj}. \quad (51)$$

for $-n < j \leq n$. The latter is shortly written as:

$$a^{(k)} = \mathcal{F}[h^{(k)}], \quad (52)$$

where \mathcal{F} denotes the Fourier transform, which will be chosen as the Fast Fourier Transform (FFT) algorithm, thus imposing that n is an integer power of 2. The intermediate mapping $\omega^{(k)}$ is computed from the $a^{(k)}$ as:

$$\begin{cases} \omega_j^{(k)} = (i/n)a_j^{(k)} & \text{for } j > 0 \\ \omega_0^{(k)} = (i/2n)a_0^{(k)} \\ \omega_j^{(k)} = 0 & \text{for } j < 0. \end{cases} \quad (53)$$

The latter form is obtained from the identification of Eq.(49b) and the definition of $a^{(k)}$, taking care of the fact that one sum is over positive index, while the other extends over the interval $[1-n, n]$. Then, one computes

the series:

$$\begin{cases} b_j^{(k)} = ia_j^{(k)} & \text{for } j > 0 \\ b_0^{(k)} = 0 \\ b_j^{(k)} = \overline{b_{-j}^{(k)}} = -i\overline{a_{-j}^{(k)}} = -ia_j^{(k)} & \text{for } j < 0. \end{cases} \quad (54)$$

This linear transformation is shortly noted as:

$$b^{(k)} = \mathcal{H}[a^{(k)}], \quad (55)$$

where \mathcal{H} is the above detailed transformation. The form of \mathcal{G} is dictated by Eq.(49a) for positive index, and from the fact that the inverse Fourier transform of b (see below) is real. The new sampling series is finally obtained from:

$$u_j^{(k+1)} = \frac{j\pi}{n} + \mathcal{F}^{-1}[b^{(k)}]. \quad (56)$$

The equations (50-56) define one step in the algorithm relating $\omega^{(k+1)}$ to $\omega^{(k)}$. We note this step $\omega^{(k+1)} = \mathcal{T}(\omega^{(k)})$. The searched function Ω is clearly a fixed point of the transformation \mathcal{T} defined above in a discretized version. The uniqueness of the transformation Ω results from that of the harmonic field in the domain \mathcal{E} with an equipotential condition on the boundary and a constant gradient perpendicular to the boundary at infinite distance from it. Therefore, the only condition to consider is the stability of the fixed point. As it can be seen in Ref. [1], this fixed point is attractive at the only condition that:

$$\max |h'(u)| < 1. \quad (57)$$

The procedure described above gives a very fast and efficient way of building conformal mappings. It has to be noted indeed that this two-dimensional problem is solved here by the only use of a few one-dimensional fast Fourier transforms. In cases of slopes locally overcoming one, it is possible to use under-relaxation schemes (see details in Ref. [2, 4]) or to decompose the mapping in several substeps such that the convergence criterium is always fulfilled.

-
- [1] D. Vandembroucq and S. Roux. *submitted to Phys. Rev. E*, 1996.
- [2] M.H. Gutknecht. *Numer. Math.*, 36:405, 1981.
- [3] P. Henrici. *Applied and Computational Complex Analysis*, volume III. Wiley Classics, New York, 1993.
- [4] M.H. Gutknecht. *SIAM J. Sci. Stat. Comput.*, 4(1):1-30, 1983.
- [5] B. B. Mandelbrot, D. E. Passoja, , and A. J. Paullay. *Nature*, 308:721, 1984.
- [6] E. Bouchaud, G. Lapasset, and J. Planès. *Europhys. Lett.*, 13:73, 1990.
- [7] K. J. Måløy, A. Hansen, E. L. Hinrichsen, and S. Roux. *Phys. Rev. Lett.*, 3:213, 1992.
- [8] J. Schmittbuhl. PhD thesis, Univ. Paris VI, 1994.
- [9] F. Plouraboué. PhD thesis, Univ. Paris VII, 1996.
- [10] E.O. Tuck and A. Kouzoubov. *J. Fluid Mech.*, 300:59, 1995.
- [11] S. Richardson. *J. Fluid Mech.*, 59(4):707, 1973.
- [12] J.J.L. Higdon. *J. Fluid Mech.*, 159:195, 1985.
- [13] K.M. Jansons. *Phys. Fluids*, 31:15, 1988.
- [14] C. Pozrikidis. *J. Fluid Mech.*, 255:11, 1995.
- [15] C. Pozrikidis. *Boundary Integral and Singularity Methods for Linearized Viscous Flow*. Cambridge University Press, Cambridge, 1992.

- [16] E. Guilloteau. PhD thesis, Univ. Paris-Sud, 1995.
- [17] W.A. Weibull. *Proc. Roy. Swed. Inst. Eng. Res.*, (151), 1939.
- [18] D. Vandembroucq and S. Roux. unpublished, 1996